Performance Analysis of HD1: A 16 Tesla Nb_3Sn Dipole Magnet

S. Mattafirri, S.E. Bartlett, P.A. Bish, S. Caspi, D.R. Dietderich, P. Ferracin, S.A. Gourlay, C.R. Hannaford, A.R. Hafalia, W.G. Lau, A.F. Lietzke, A.D. McInturff, M. Nyman, G.L. Sabbi, R.M. Scanlan

Abstract—The Superconducting Magnet Group at Lawrence Berkeley National Laboratory (LBNL) has been developing technology for high field accelerator magnets from brittle conductors. HD1 is a single bore block dipole magnet using two, double-layer Nb_3Sn flat racetrack coils. The magnet was tested in October 2003 and reached a bore peak field of 16 T (94.5% of short sample). The average quench current plateau appeared to be limited by "stick slip" conductor motions. Diagnostics recorded quench origins and preload distributions. Cumulative deformation of the mechanical structure has been observed. Quench velocity in different field regions has been measured and compared with model predictions. The results obtained during the HD1 test are presented and discussed.

***Index Terms*— Nb_3Sn superconducting dipole, quench origin, quench propagation, quench protection.**

I. Introduction

HD1 was designed, manufactured and tested at LBNL as part of the R&D program on high field magnets for next generation particle accelerators. The magnet, a Nb_3Sn dipole with two double-layer flat racetrack coils, was tested for the first time in October 2003 and reached a bore peak field of 16 T (94.5% of the calculated short sample limit assuming no degradation due to cabling or stress effects). The average calculated pre-stress on the brittle conductor is 155 MPa. A second test in a different pre-stress configuration was performed in May 2004 (HD1b) [1].

A first report of the test results has been previously presented [2]. This paper is reporting further data analysis results on the quench origin and pre-stress distribution, cumulative deformation of the mechanical structure, quench velocity and quench protection.

II. Magnet Features and Test Set Up

The cross-section of HD1 is shown in Fig. 1. Details on the mechanical structure, design, manufacturing and conductor, have been previously presented [3]. It is relevant to mention that HD1 was assembled with a 3D pre-stress configuration using key and bladder technology and axial aluminum rods.

Manuscript received October 4, 2004. This work was supported under contract DE-AC03-76SF00098 by the Director, Office of Energy Research, Office of High Energy Physics, U.S. Department of Energy.

All Authors are with Lawrence Berkeley National Laboratory, Berkeley, CA 94720 (phone: 001 510 486 4042; fax: 001 510 486 5310; e-mail: SMattafirri@lbl.gov).

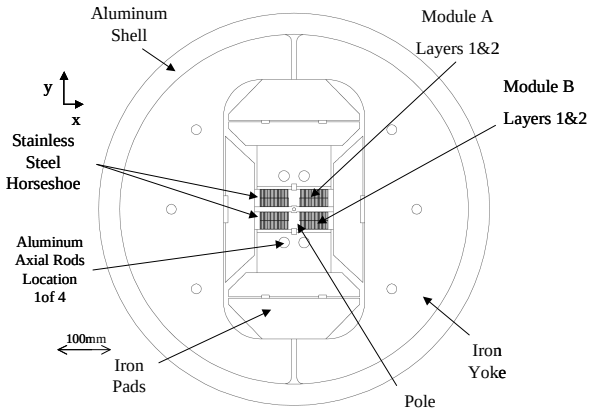

Fig. 1. HD1 cross section.

The axial pre-stress was necessary to constrain the conductor displacements in the ends due to longitudinal Lorentz forces.

The Rutherford cable (1.36 x 15.75 mm^2) is composed of 36 - 0.8 mm diameter strands and is insulated with S-glass sleeve. The cable was wound around the iron pole in a double layer configuration, heat treated and impregnated [3]. The heat treatment resulted in a measured RRR of 15 and J_c>3000 A/mm^2 @ 12T and 4.2K.

Quench origins and propagation were detected using 11 voltage taps per layer. The voltage tap pairs were located strategically to monitor, in particular, the layer to layer transition and the turns next to the mechanical structure (island, spacers, horse shoe).

The stored energy is 0.45 MJ at short sample. The magnet was actively protected by laminated quench heaters to avoid high local peak temperatures and high internal differential electrical potential during quench. Each coil layer was equipped with a 0.3 ohm quench heater, impregnated in contact with the coil, which covered 65% of the turns on both sides of the winding island. The heater elements are made of ~23 μm thick Stainless Steel press-glued on a ~25 μm Kapton sheet for electrical insulation. A dump resistor was available to facilitate current decay and adjusted to keep the voltage between the magnet leads below 500 V. Fig. 2 shows one of the two outer layers, the quench heater and the 9 voltage tap trace (the 2 voltage taps across the splice are not shown).

Constantan temperature compensated strain gauges were used to monitor the mechanical structure strain/stress during assembly, cool down, Lorentz force loading and warm up. Nine half-bridge type strain gauges were used along the azimuthal and axial direction on the aluminum shell and one

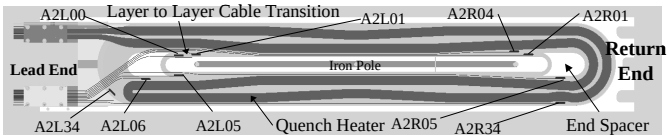

Fig. 2. Coil module outer layer. The inner layer is a mirror image of the outer layer and the voltage tap turn number is equal to the outer layer voltage tap turn number plus one (the inner layer has one turn

full-bridge type gauge on 2 of the 4 axial aluminum rods.

III. Quench Performance

A. Training

The training characteristic of HD1 at 4.5 K is shown in Fig.

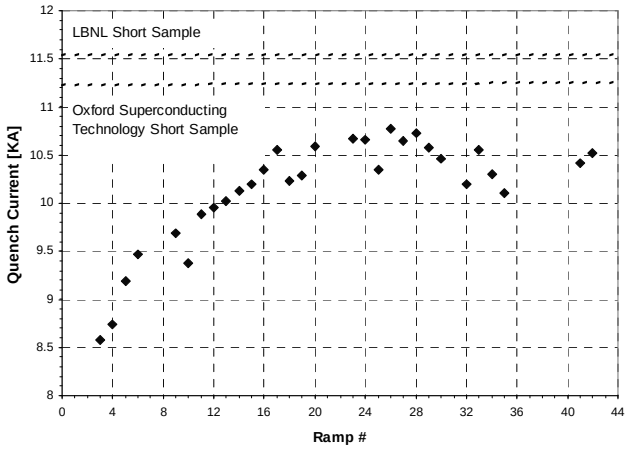

Fig. 3. HD1 training curve at 4.5 K.

3. Training considerations are presented in [1, 2].

Several fast flux changes were recorded while ramping the current. Among those, some "low frequency" flux imbalances [1] triggered the quench protection system at currents as high as 8.6 kA (ramp #3). An imbalance detection threshold of 1.5 V was needed to avoid tripping on such non-transition spurious events.

B. Quench Origin

Each voltage tap pair signal was monitored through a calibrated derivative amplifier and sampled at 5 kHz.

Fig. 4 shows a dV/dt signal developing at quench onset, and one of the two quench fronts escaping the next adjacent voltage tap after a few ms. In most cases, the time of flight was clearly identified because it was smaller than the current extraction delay and the time needed to initiate distributed quench with the quench heaters (only for the last two quenches, ramp #41 and #42, this condition did not occur). The quench origin was thus determined using a time of flight technique [4]. The dV/dt signal was analyzed to obtain the quench velocity, as described in the following section, and then multiplied by the time of flight to compute the location of the quench origin from the voltage tap.

Fig. 5 shows a detailed quench origin map. The first 20 training quenches originated at the ends, 15 of them next to the return end spacer, 3 next to the lead end spacer, and 2 next to the pole in the return end. When the quench originated next to the return end spacer, the inner and outer layers quenched within 5ms of each other (Fig. 4), and ~10% of the times

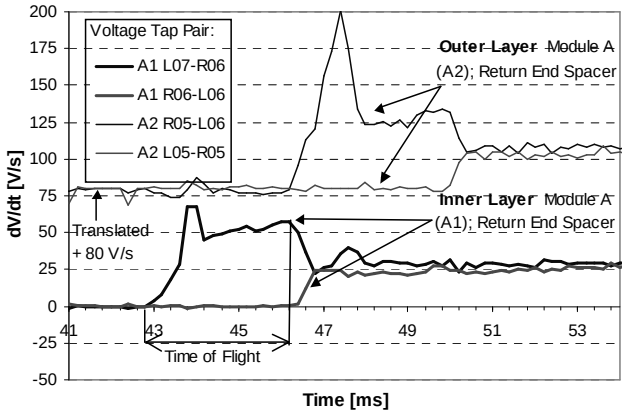

Fig. 4. Analog dV/dt signals developing at quench onset and propagation. The quench originates at 42.8 ms in the inner layer of module A on the turn next to the return end spacer. After 3.4 ms a quench develops in the outer layer of module A, on the turn next to the return end spacer.

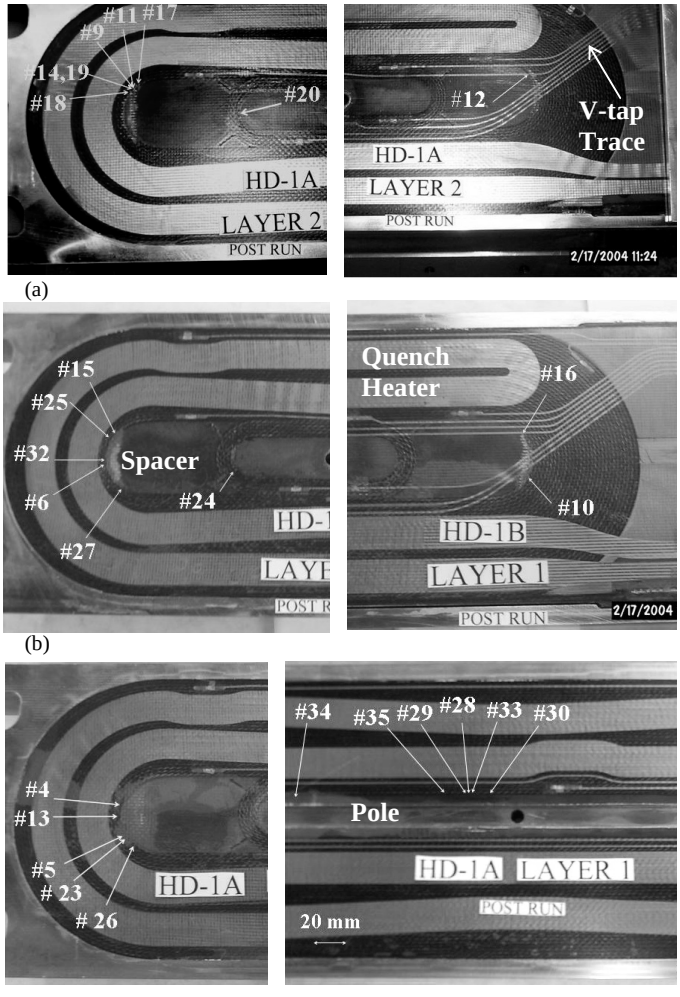

Fig. 5. Quench origin and quench I.D. (ramp #); (a) module A outer layer, return end (left) lead end (right); (b) module B inner layer, return end (left), lead end (right); (c) module A inner layer, return end (left), straight section (right).

simultaneously. The quench origin moved to the pole straight section at ramp #28. The last 2 quenches, following ramp rate studies [2], originated in the pole on the opposite side of the ramp.

A large number of quenches originated in the ends (low field region), and in the turn adjacent to the outer surface of the

spacer. Mechanical analysis shows a gap opening up in this area between conductor and spacer during Lorentz force loading [5]. Furthermore, for most of the quenches that originated in the ends, diagnostics recorded "high frequency" fast flux imbalances [6] a fraction of ms before quench onset. Both facts are consistent with an axial slippage as a heating mechanism for the quenches originating at the ends. It is yet unclear why the majority of the quenches, which originated in the ends, occurred in the return end side.

A pressure sensitive paper test was performed after magnet warm up and disassembly to check preload distribution. The "Fuji" paper trace revealed non-uniformity with a lower preload in the straight section, around the area where most of the straight section quenches occurred [5].

IV. Quench Propagation

At quench onset the dV/dt signal showed the initial transition "spike" of less than 2 ms duration, and then a slightly increasing value due to resistivity rise with temperature (Fig. 4). The longitudinal quench velocity was evaluated using the dV/dt value right after the transition "spike". A constant current and temperature was assumed for this stage. The value used for the Cu resistivity is the value measured during magnet warm up at the transition and adjusted (for magneto resistance effects) based on the calculated magnetic field in the conductor at quench onset.

The measurements are compared with the velocity calculated using an analytical adiabatic model [7]. The model uses density, thermal conductivity and specific heat weighted over the Cu, Nb_3Sn and epoxy content in the cable; the current density is computed over the Cu area in the cable, and the resistivity is the Cu resistivity for a RRR of 15, at the calculated magnetic field where the quench originated. All the material properties are at the average temperature between T_c and T_{cs} (critical temperature and temperature of current sharing). The T_c and T_{cs}, are computed applying Summer's parameterization [8] to the current density and magnetic field in the conductor at quench onset.

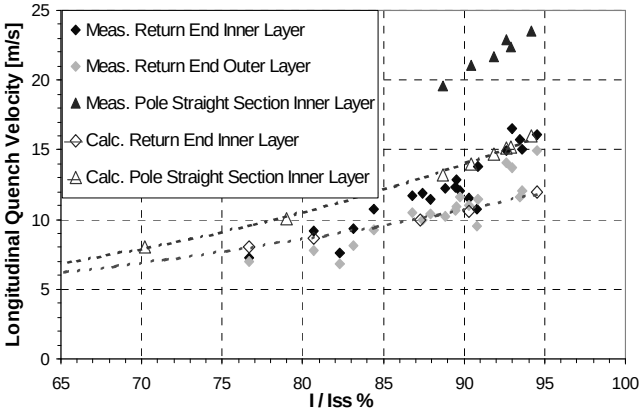

Fig. 6. Longitudinal quench velocity, measured and calculated

The measured and calculated quench velocity is shown in Fig. 6 as a function of the quench current for each coil region where quenches originated. The calculated magnetic field at 94% of short sample in the pole straight section (inner layer), and in the return end inner and outer layer, is respectively 14.6 T, 12.5 T and 11.6 T. The calculations show a departure from the measurements increasing with quench current. The departure is more evident for the pole straight section.

V. Quench Protection

The delay of the protection heaters from the quench detection was set to a standard time of 10 ms and the current extraction delay was set to 40 ms. This choice was a compromise between quench propagation analysis and magnet protection issues. The quench heaters were powered by two independent power supplies for redundancy. Each one of the power supplies was connected to the quench heaters (in series) in electrically non-adjacent coil layers. This choice limits the internal peak voltage in case of failure of one of the two power supplies.

The peak temperature has been evaluated after each quench. With the standard protection systems delays, the measured MIITS ranged from 5.30×10^6 A^2sec to 7.23×10^6 A^2sec depending on quench propagation, quench current and quench detection delay. At ramp #33, 34 and 35, the protection heater delay was progressively increased until they were powered long after the current extraction; the extraction delay was still 40 ms.

Table 1 summarizes some quench protection parameters for the two different conditions: quench heaters powered before extraction and after extraction.

The peak temperature in function of the MIITS was evaluated, considering the heat balance of a unit volume of winding in adiabatic conditions using the program QUENCH [7]. The maximum peak temperature was 119 K. The peak temperature differs by 18 % when the quench heaters are powered before extraction and after extraction.

TABLE I
QUENCH PARAMETERS FOR DIFFERENT QUENCH PROTECTION SETTINGS

Quench I.D. [Ramp #]	# 15	# 32	# 34	# 35
Protection Heaters Delay [ms]	16	16	74	105
Current Extraction Delay [ms]	50	50	50	45
MIITS[(1)] [10^6 A^2 sec]	7.23	6.85	8.85	8.81
T peak[(2)] [K]	105	101	119	119
Internal **ΔVmax**[(1)] at Extraction [V]	130	125	150	150

[(1)]Measured; [(2)]Calculated.

VI. Residual Strain of the Mechanical Structure

The azimuthal stress in the aluminum shell and the axial stress in the aluminum rods increased significantly during cool down (90 MPa in the shell and 135 MPa in the rods).

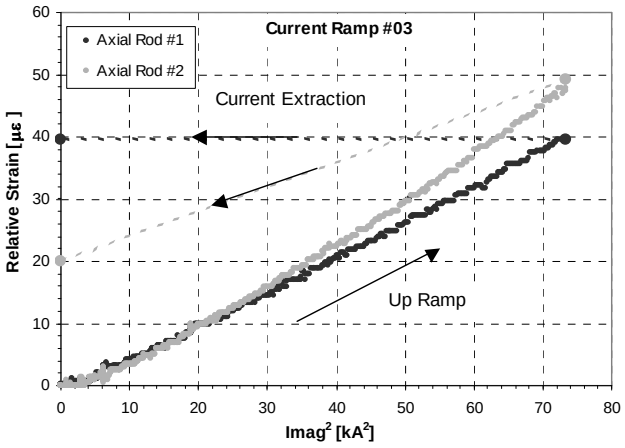

Fig. 7. Strain variation during Lorentz force loading and after unloading.

Fig. 7 shows the strain response in the aluminum axial rods during and after a current ramp. Comparisons between measurements and calculations are discussed in [5]. This particular ramp (#3) was the first above 2 kA and no quench occurred (the current extraction was triggered by a "low frequency" flux imbalance). After the Lorentz force vanishes, the strain in the mechanical structure is measured to be different than the original unloaded condition. A positive residual strain is measured for the axial rods, and a negative one is measured for the shell (not shown).

The phenomenon has been investigated for all the current ramps and the results are summarized in Fig. 8.

Cumulative residual deformation of the mechanical structure, in the axial direction, has been previously observed in some SSC magnets [9], yet the cause is not fully understood.

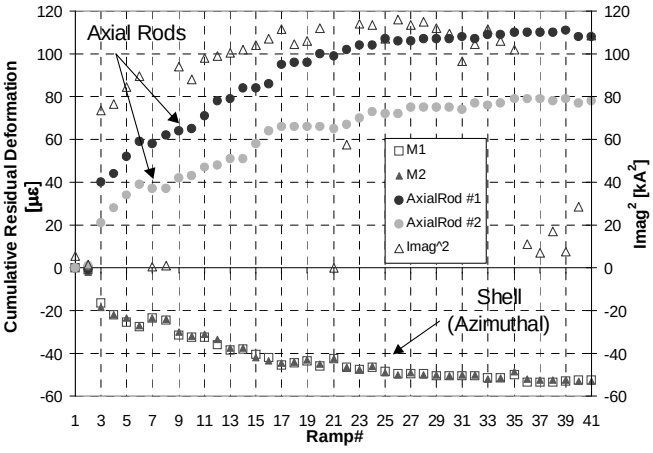

Fig.8. Residual cumulative deformation of the mechanical structure (strain after current ramp # n – strain before the beginning of the first current ramp).

Friction could explain a cumulative residual deformation if the friction force was increasing at each cycle. However strain variation is measured since the beginning of the ramp and no significant change in slope during the loading phase is detected for all the cycles. Results show that: (a) most of the residual deformation is obtained after the first loading cycle; (b) residual deformation occurs after each current ramp exceeding the maximum current obtained in previous cycles; (c) very little residual deformation (or none) occurs after "fall back" quenches or current ramps.

This phenomenon suggests that, after Lorentz force unloading, the coil might be in a tension strained status in the axial direction and in a compression strained status in the x direction. The results of related further experiments made with Nb_3Sn sub-scale coils equipped with strain gauges are discussed in [10].

VII. Conclusions

The HD1 test results, in line with the mechanical analysis, suggest that the coils were not adequately supported along the axial direction. Furthermore, a normal pre-stress non-uniformity, with low pre-stress regions along the magnet axis, seemed to be the cause of the straight section region premature quenching. Both problems have been addressed with a second HD1b preload configuration. It is still not clear why most of the end quenches occurred in the return end side.

The peak temperature calculated in adiabatic conditions from the MIITS measurements never exceeded 119 K.

The longitudinal quench velocity measured in different magnetic field regions and at different quench currents, up to 94.5% of short sample, ranges from 7.0 m/s to 23.5 m/s.

A 3D cumulative residual deformation of the structure, during training, increased the strain in the axial rods ~90 με and decreased the azimuthal strain in the shell ~50 με.

References

[1] A. F. Lietzke *et al.*, "Test Results of HD1b, an Upgraded 16 Tesla Nb_3Sn Dipole Magnet", *This Conference Proceedings*.

[2] A. F. Lietzke *et al.*, "Test Results for HD1, a 16 T Nb_3Sn Dipole Magnet", *IEEE Trans. Appl. Superconduct.*, vol. 14, n 2, June 2004.

[3] A. R. Hafalia *et al.*, "HD1: Design and Fabrication of a 16 T Nb_3Sn Dipole Magnet", *IEEE Trans. Appl. Superconduct.*, vol. 14, n 2, June 2004.

[4] A. Devred *et al.*, "Quench Start Localization in Full Length SSC R & D Dipoles." Presented at 1st Int. Industrial Symp. on the SSC, New Orlans, LA, Feb 8-10, 1989. Published in New Orleans IISSC 1989.

[5] P. Ferracin *et al.*, "Mechanical analysis of the Nb_3Sn dipole magnet HD1", *This Conference Proceedings*.

[6] L. Chiesa *et al.* "Performance Comparison of Nb_3Sn Magnets at LBNL", presented at ASC02, August 2002, Houston USA, *IEEE Trans. Appl. Superconduct.*, vol. 13, n.2, June 2003.

[7] M. N. Wilson, "Superconducting Magnets" chapter 9, 1st published Oxford Science Publication, 1983.

[8] L. T. Summer *et al.*, "A Model for the Prediction of Nb_3Sn Critical Current as a Function of Field, Temperature, Strain and Radiation Damage", *IEEE Trans. Magn.*, vol. 27, no. 2, 1991, pp. 2041-2044.

[9] A. Devred *et al.*, "The Mechanics of SSC Dipole Magnets", *AIP Conf. Proc. 249*, vol.2, pp1367, 1992.

[10] S. Caspi, *et al.*, "Measured Strain of a Nb_3Sn Coil During Excitation and Quench", *This Conference Proceedings*.